COBEM 2023 27TH INTERNATIONAL CONGRESS OF MECHANICAL ENGENEERING

ABCM Brazilian Society of Mechanical Sciences and Engineering
27th ABCM International Congress of Mechanical Engineering
December 04-08, 2023, Florianópolis-SC, Brazil

COB-2023-0423
THE TRANSITION OF RESEARCH REACTOR FUELS FROM DISPERSION TO MONOLITHIC FUEL

Daniel de Souza Gomes
Instituto de Pesquisas Energéticas e Nucleares (IPEN), Av. Professor Lineu Prestes 2242, São Paulo, SP, Brasil
dsgomes@ipen.br

Abstract. *Research reactors function as neutron sources for studies and do not produce electricity. Over the past 70 years, they have significantly contributed to the progress of nuclear science, encompassing material development, the production of radioisotopes, and many other fields. Today, there are 222 reactors in operation in 53 countries. Until 1978, the concept of compact nuclei prevailed, producing a high flux of neutrons based on highly enriched uranium plates. Today's standard is dispersion fuels, with a low enrichment below 20% of U-235. These units operate with a thermal neutron using light water as a coolant, sometimes graphite as the moderator, and beryllium as the reflector. Uranium-aluminum alloys were the first fuels manufactured in plate form in the 1950s. U_3O_8 dispersed in aluminum and clad with an aluminum alloy, U_3O_8/Al, started in the 1960s. Since 1978, there has been an impetus to reduce 235-U enrichment, changing to UAl_x-Al with a high uranium load. Following the same idea arose U_3Si_2/Al and U10Mo/Al of up to 4.8 gU/cm^3, and in the 1990s, 6.0 gU/cm^3. During the 2000s, this loading increased to 16.3 gU/cm3 using U-7Mo monolithic fuel. Dispersed and monolithic fuels' physical and thermal features define their application fields.*

Keywords: *U_3Si_2/Al, U-10Mo/Al, dispersion fuels, critical flow velocity.*

1. INTRODUCTION

Around the world, a few high-performance research reactors are in operation, working with highly enriched uranium (HEU: ≥20% U-235). A global effort is underway to minimize and eliminate HEU's use. About 70 reactors converted from HEU to low-enriched uranium (LEU: <20% U-235). However, the engineering task for conversion is very complex. Also, it needs the development and qualification of new high-density fuels, such as U_3Si_2/Al, U-Mo/Al, and U-Mo monolithic fuel (Mariani et al., 2020). It is necessary to enhance the uranium density in the fuel in order to make up for lost enrichment when creating low-enriched fuels to replace high-enriched fuels for these reactors.

Nuclear fuels are materials capable of producing energy through the self-sustaining nuclear fission reaction. Fissile materials such as U-235 and U-233 are fundamental to manufacturing nuclear fuels. Over the years, material test reactors (MTRs) have employed dispersion fuel plates using an aluminum matrix. Fuel plates must contain fissile material dispersed in aluminum powder to form a fuel core. Forming a zone fuel, so-called meat fuel, and two aluminum alloy sheets cladding the meat (Iltis et al., 2023). An assembly of regularly spaced aluminum fuel plates makes up the MTR fuel element. These areas enable a stream of cooling water to flow through them. The fissile materials U-235 and U-233, which contain meat, are in the center of the plates and covered in aluminum. The manufacturing process for fuel plates is based on metallurgical powder. They then placed briquettes for dispersion fuel inside a frame covered in aluminum plates, which must be welded before rolling. First, MTRs used uranium dioxide (UO_2) and triuranium octoxide (U_3O_8). In the 1990s, MTRs used uranium silicide dispersion (U_3Si_2/Al) and uranium molybdenum dispersion (U-7Mo/Al) after 2000. Commercial nuclear reactors have also operated with uranium carbides (UC) and uranium mononitride (UN) (Pioro et al., 2022).

The evolution of dispersion fuel shows at least three phases. In the first generation, the fuel plates started with the U-Al alloy fuel system in the 1950s. However, uranium loading on the fuel plates had its limits, which increased in the 1960s. UAl_x-Al dispersion fuel increased uranium densities from 30% to 50% (Konings and Stoller, 2020).

However, uranium loading on the fuel plates had its limits. During the 1960s, enhanced uranium densities increased between 0.4 and 0.8 gU/cm^3, with peak densities of 1.7 gU/cm^3. The Savannah River reactor introduced the dispersion of uranium-aluminide powder dispersed in an aluminum matrix (UAl_x-Al) (Konings & Stoller, 2020). They have also used uranium oxide powder dispersed in an aluminum matrix (U_3O_8-Al) with densities up to 1.3 g/cm^3. In 1980, uranium densities for U_3Si_2/Al (77% weight of U_3Si_2) achieved 3.7 g/cm^3 and improved to 4.8 g/cm^3. In the 1990s, U_3Si_2/Al achieved 12.2 g/cm^3 (Chandler et al., 2019; Mei et al., 2019; Wang & Xu, 2004). Since 1990, metallic U-Mo alloy fuels have been one of the more adequate fuels (Rest et al., 2011).

The manufacturing standard route is the picture frame technique (PFT) used to produce fuel plates. PFT uses two Al alloy foils to enclose meat fuel submitted to hot rolling processing to make a set of reduced thicknesses. First, through induction melting and annealing of uranium metal with Al, Si, and Mo, followed by a metallurgic powder route. After the execution of powder phases, such as crushing, grinding, and screening, fuel particles range in size from 44 to 150 microns.

After the fuel zone, use a picture frame encasing the fuel meat. In the next step, it wrapped the meat fuel in two aluminum plates and welded them to the edges of the plates, following hot and cold lamination to merge the cladding. At first, uranium-aluminum alloys used pure aluminum, which operated under irradiation for over fifty years.

Argonne National Laboratory (ANL) established the Reduced Enrichment for Research and Test Reactor (RERTR) program in 1978 to replace highly enriched uranium (HEU > 20% U-235) with low-enriched uranium (LEU < 20% U-235). In this epoch, research is underway to change HEU to LEU, and the most promising fuels are gU (Mo) and U_3Si_2. In 2016, the American Defense Nuclear Nonproliferation (DNN) agency substituted the RERTR program for Materials Management and Minimization (M3). Within the M3 goals, we have the conversion of HEU (useable for weapons) to LEU.

Since 1985, the growth of uranium silicide dispersion has been notable, based on U_3Si and U_3Si_2. As a function of silicide-Al dispersion, it has a higher thermal conductivity than U_3O_8-Al. Besides, it increases their principal advantage of uranium density. Again, silicide dispersion has substantial corrosion resistance in hot water. Then, U-7Mo dispersion replaces silicides and includes U-10Mo monolithic fuel designs. Molybdenum is an element that, even in low concentrations, can maintain the gamma phase of uranium, stabilizing the fuel element during the manufacturing process and when irradiated. In U-Mo alloys, the stabilized gamma phase helps to develop fuels with a higher uranium density.

At the turn of the millennium, a few European irradiation programs ensured the qualification of dispersion plates. The IRIS irradiation plan showed three phases performed at the core of the Osiris French reactor at a maximum heat flux of 240 W/cm^2. European programs ensured the qualification of UMo. FUTURE was the UMo irradiation plan performed in the Belgian Reactor 2 (BR2) reactor at a higher peak heat level of 350 W/cm^2 (Leenaers et al., 2017). The E-FUTURE test presented following this one had a maximum heat output of 470 W/cm^2. In 2012, European irradiation tests used plates made of LEU with U-7wt% Mo dispersed in aluminum containing 4% to 6% silicon. U-Mo/Al-Si, operated with a density of 8 gU/cm^3 using the surface engineering of low-enriched uranium molybdenum (SELENIUM) program.

In this context, in Brazil, there are four research reactors in operation: the IEA-R1 and the MB-01 reactors, both at the Nuclear Energy Research Institute (IPEN, São Paulo); the Argonauta at the Nuclear Institute of Nuclear Engineering (IEN, Rio de Janeiro); and the IPR-R1 reactor at the Nuclear Technology Development Center (CDTN, Belo Horizonte). The IEA-R1, supported by the nuclear institute IPEN, located in São Paulo, is in operation and had its first criticality in 1957. It has a thermal neutron flux of 4.6×1013 n.cm-2.s-1 and a fast flux of 1.3×10^{14} n/cm^{2}s in a steady state. The Training, Research, Isotopes, and General Atomics (TRIGA) IPR-R1 reactor was the second research reactor installed in Brazil. IPR-R1 works at 100 kW but will operate at 250 kW.

This study investigates the dispersion fuel used in research and test reactors. It also helps to determine the suitable options for the aluminum matrix and metallic fuel, such as ceramic and ceramic-metal dispersion. The main aim was to assess the complementary concepts of dispersion and monolithic fuel and describe state-of-the-art fuel plate technology.

2. DEVELOPMENT OF DISPERSION FUELS PROGRESS

Uranium shows three crystalline forms: orthorhombic, tetragonal, and gamma phase, from 25 °C to 1132 °C. The orthorhombic uranium phase had four atoms per unit cell (Kim et al., 2006). However, the alpha (orthorhombic) phase is notorious for having poor dimensional stability at low temperatures, leading to anisotropic behavior. While γ-U is stable from 760 °C to 1133 °C, it also shows an isotropic response and less swelling during irradiation.

Various alloying elements, including molybdenum, niobium, and zirconium, stabilize the gamma phase (body-centered cubic). Phase transformation (α-β) occurs at 667 °C (Bobkov et al., 2008; Frazer et al., 2021). The tetragonal-beta phase is stable from 667 °C to 775 °C. In the second phase transition, (β-γ) at 775 °C The body-centered cubic (BCC) of the gamma phase reduces volume and is stable between 775 °C and 1132 °C.

Over the years, the research reactors adopted uranium intermetallic fuels, such as U-Al, U-Si, and U-Mo. Metals like Zr, Si, Al, Nb, Mo, Cr, V, and Ti can compose uranium metal alloys, divided into two classes. In the first class, metals that permit beta-phase at room temperature, such as V, Nb, Cr, Mo, and Mn. Then, the second class has metals such as Nb, Mo, and Zr, which permit the gamma phase at room temperature. However, retaining the gamma phase is possible using metals of Groups V through VIII (Hofman et al., 1998). However, uranium metal has poor irradiation stability and has the highest uranium density, but it needs extended usability. For six decades, around the world, many tests and research reactors used dispersion fuel. The U-Mo/Al dispersion fuels can replace the highly enriched uranium (HEU) fuels in many research reactors. U-Mo/Al contains spheres of u-MO with 50–75 microns dispersed in the Al matrix. Then, encapsulate the combustible meat on both sides with aluminum plates to produce a fuel element. UMo/Al shows the disadvantage that U-Mo fuel particles chemically interact with the Al matrix.

Consequently, it forms an interaction layer of low thermal conductivity between uranium and aluminum. The reduced thermal conductivity will produce fuel swelling. (Williams et al., 2013).

The MTR fuel plates comprise a fuel core or meat covered in aluminum alloy cladding. UAl_3 and UAl_4 are wrought alloys of uranium and aluminum precipitated in an aluminum matrix (Kniznik et al., 2011). Fission density has a linear relationship with irradiation, swelling, and the release of fission products. However, the process by which fission gas swells is complex. The gas atom diffusion inside the fuel grain directly impacts how much the fission gas swells. Figure 1 represents the dispersion plate fuel.

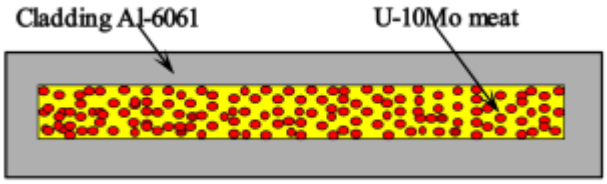

Figure 1. U-10Mo dispersion in aluminum.

During the 1950s, HEU fuels started with monolithic U-Al fuels that contained about 15 wt% of U. Also, it produced LEU fuel plates, including 48 wt% of U-235. Aluminide (UAl_x) is a mixture of UAl_2, UAl_3, and UAl_4 used in type dispersions (UAl_x-Al). In the 1960s, the intermetallic UAl_x represented high uranium density, high thermal conductivity, and low neutron absorption (Kniznik et al., 2011).

Research has arisen about ceramics: UO_2, U_3O_8, UC, UN, and U_3Si_2 dispersed in aluminum. Radioisotope production uses UAl_x aluminides as targets to produce 99Mo. During the 1960s, U_3O_8 was the most stable form of uranium oxide. The Oak Ridge National Laboratory (ORNL) and Argonne National Laboratory (ANL) introduced the manufacturing route for U_3O_8 powder because it was the most stable state of uranium oxides in the 1960s (Copeland et al., 1982). The metal powder metallurgy (PM) process produces U_3O_8-Al using hot roll bonding. The PM route creates swelling or blisters when heated above 600 °C. Besides, U_3O_8-Al fuel suffers from the effect of partial reduction on U_4O_9 on the thermic reduction reaction. Table 1 depicts a simple comparison of the physical properties of intermetallic and ceramic fuels.

Table 1. Uranium-aluminide properties used in fuel plates.

Aluminides physical properties	**UAl_2**	**UAl_3**	**UAl_4**
MP (K)	1590	1350	730
Density ρ(g/cm^3)	8.1	6.8	6.0
Uranium density ρ(U) (gU/cm^3)	6.64	5.08	4.16
Uranium content (wt%)	81.3	74.4	68.5
Formation energy ΔE (kJ/mol)	6.8	-9.3	-3.8

The RERTR program aims to eliminate the HEU fuels used in MTRs. The RERTR developed LEU fuels to replace the corresponding HEU fuels without affecting experiment performance or costs. In the 1980s, the silicide dispersion of U_3Si_2/Al began, showing densities of 3.0 to 4.5 gU/cm^3. In the 1990s, the methods to produce metallurgic powder employed machining and grinding, then incorporating the atomization process to fabricate fuel plate dispersions. In 2007, the Idaho National Laboratory tested a rotating atomizer to produce U-7Mo with a particle size of 5 μm. It has intensified efforts to industrialize monolithic U-10Mo in the last decade using a zirconium diffusion barrier and Al-6061 cladding. The monolithic design has a high uranium load that could replace the dispersions, and the qualification process is for 2021.

In the U-10Mo fuel system, molybdenum stabilizes the gamma phase of uranium. The uranium gamma phase is anisotropic, showing BCC structure. However, dispersion fuels have drawbacks, such as swelling, corrosion between U and Al, and forming an interaction layer (Kim & Hofman, 2011). Adding Si or Zr to Al-matrix improves bubble gas retention (Park et al., 2008). The growth of the interaction layer (IL) shows dependence on the fission density. The interaction layer displays low thermal conductivity, poor fission gas retention, and induces large pores.

2.1 Physical properties of dispersion fuel

Intermetallic fuels like U-Al, U-Si, and U-Mo perform better in MTRs. Where neutron production, rather than power generation, is the primary goal. Early (U-Al) alloys with high uranium contents pose difficulties during the rolling process and increase proportionally with uranium content. In the case of UO_2/Al, the limit is 25 wt% UO_2. The type of aluminum used in the Al-matrix and Al-cladding, in part, determines the physical behavior of the Al-dispersion. The U-Al_{ex} dispersion shows a low uranium content of 1.7 gU/cm^3 in the fuel meat area (37 vol% of U-Al). Silicide particles dispersed in aluminum began with U_3Si, then changed to U_3Si_2 powder, which is easier to make and requires fewer fabrication steps than U_3Si. The U_3O_8-Al dispersion fuel produced a ceramic compound with a 1.3 gU/cm^3 density in meat fuel, showing 18 vol% of U_3O_8 (Wilson et al., 2019; Yang et al., 2021).

A LEU fuel qualification was tested for UAl_x-Al, which achieved a uranium density of 2.3 g/cm^3. In contrast, U_3O_8-Al permitted densities up to 3.2 g/cm^3. Table 2 illustrates the fissile materials used to produce aluminum dispersions.

Table 2. Fissile materials are used to produce aluminum dispersion fuels.

Physical properties	**U**	**U_3O_8**	**U_3Si_2**	**U-7Mo**	**U-10Mo**	**$(U_{0.31},Zr)H_{1.6}$**	**U-7Nb**
Uranium density (Ug/cm^3)	19	8.3	11.3	17.1	16.04	3.7	15.0
Melting point (K)	1405	1423	1938	1148	1433	2172	1772
Thermal conductivity (W/mK)	27	1.66	8.5	11.2	11.3	18	21.1

Unirradiated U_3O_8 has a lower thermal conductivity of 1.66 W/mK at 333 K, but when irradiated, it changes to 2 W/mK. The space program introduced UZrH fuel in the 1960s, also used for TRIGA reactors, which has a hydrogen-to-metal ratio (H/M) equal to 1.6, showing a uranium load of up to 3.7 gU/cm^3. The same picture frame technique produces U_3Si_2/Al and U-7Mo/Al. After being extruded and cut to size, the meat fuel is covered in finned aluminum cladding, welded, and hermetically sealed. This picture frame manufacturing route uses Al-6061 alloys that suffer a hot-roll bond. The thermal conductivity of Al-6061 is around 160 W/mK, which decreases as uranium increases. When uranium content reaches 70 wt.%, the thermal conductivity drops to 20 W/mK. (Jian and Ding, 2020), Figure 2 shows the thermal conductivity of uranium, U-7Mo, and U-10Mo.

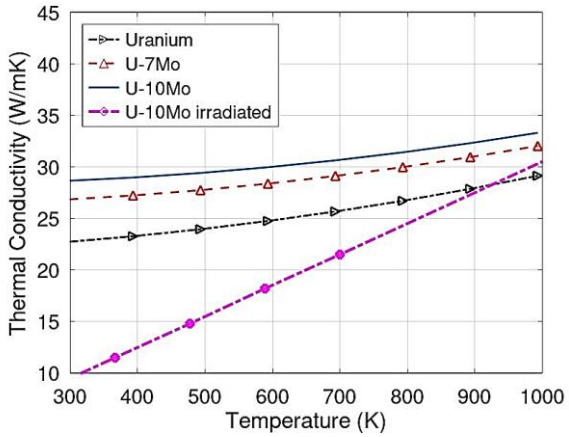

Figure 2. Thermal conductivity of uranium versus temperature.

The thermal conductivity of U_3Si_2/Al dispersions likewise depends on uranium content and porosity. Also, particles (U-Mo) dispersed in an Al-matrix determine the meat's thermal response. The thermal conductivity of Al-6061 is 167 W/mK, the interaction layer is 5.5 W/mK, and that of U_3Si_2 is 8.49 W/mK at 100 °C. Comparatively, U-10Mo shows a conductivity of 15.8 W/mK at 100 °C. Thus, with U_3Si_2/Al containing 20 wt.% of U_3Si_2, the conductivity is 90 W/mK. When it reaches 50 wt.%, the conductivity is 22 W/mK. For U_3Si, the thermal conductivity at 20 wt.% is 120 W/mK and drops to small values at 50 wt.%. Figure 3 displays the thermal conductivity of common materials used in dispersions.

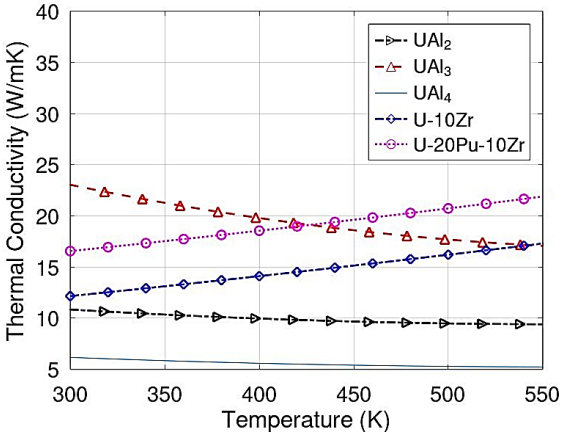

Figure 3. Thermal conductivity of metallic fuels.

In contrast, U-Mo monolithic foils have a high 18 g/cm^3 density and a thermal conductivity of over 15 W/mK. Fuel plate types show swelling as a burnup function because of fission gas release, which comprises xenon and krypton. Intermetallic fuels such as U-Mo/Al and U_3Si_2/Al show relatively low swelling. However, the swelling of U-Mo/Al alloys is more significant than that of U_3Si_2/Al. Figure 4 displays the linear coefficient of thermal expansion (CTE) of materials used in dispersions.

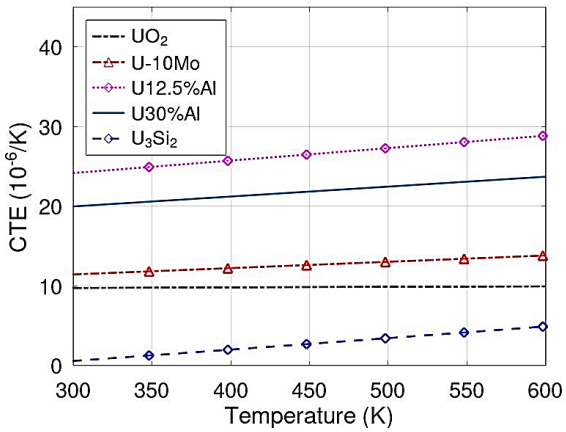

Figure 4. Linear thermal expansion of fuels used in dispersions.

It made the cladding on dispersion fuel plates of aluminum alloys. Americans adopted the Al-6061 alloy for cladding and matrix. In contrast, Canadians, French, and Russians work with other alloys, such as Al-1060, Al-6101, Al-4043, AG3NE or Al-5754, and AlFeNi, similar to Al-8000. Table 3 depicts a few properties of the uranium-aluminide compounds on the fuel plates.

Table 3. Aluminum alloys employed for dispersions: U_3Si_2-Al and U-10Mo/Al.

Physical properties	**Al-1100-H18**	**AG3NE**	**Al-6061-T6**	**Al-6101**
Melting point (K)	916-930	902-927	855-924	894-927
Thermal conductivity (W/mK)	222	130	167	218
Heat capacity (J/kgK)	904	870	896	895
CTE (10^{-6}·K^{-1})	23.6	21.9	23.6	21.7
Modulus of elasticity (GPa)	68.3	68.9	68.9	68.9
Yield tensile strength (MPa)	145	159	276	193

The INL performed an irradiation test using the Advanced Test Reactor (ATR). Plate fuel U_3Si_2/Al achieved an average heat flux of 270 W/cm^2. As a result, it produces a dense oxide layer added to a granular layer (Gan et al., 2011). Figure 5 exhibits the specific heat capacities of U-Al dispersion components.

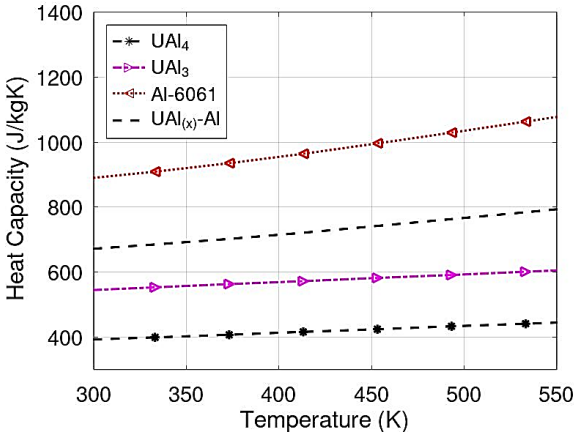

Figure 5. Heat capacity of components of plate fuel type UAl_x.

In the 1950s, the Russians used U-9Mo/Mg dispersion fuel enclosed between two stainless steel tubes. In the late 1990s, many experiments using U-Mo particles dispersed in an aluminum matrix resurfaced. Initially, U-7Mo/Al flowed by U-10Mo/Al, increasing the 6.5 gU/cm^3 uranium load to 8.5 gU/cm^3.

The aluminum oxidation produces boehmite (AlO(OH)) and bayerite (Al(OH)3). Aluminum oxides like boehmite have a low thermal conductivity of around 2.25 W/mK. Thus, the pitting corrosion and chemical reactions help to produce IL. After the fuel-Al interaction, a sizable portion of the Al matrix is increased. U_3Si_2 and U_3Si have a thermal conductivity of ~15 W/mK. The average thermal expansion coefficients of U_3Si_2 and U_3Si from 20 °C to 600 °C are 15.2×10^{-6} and 15.8×10^{-6} per K, respectively. Since the 1980s, many irradiation tests have been performed using U_3Si_2/Al dispersion fuels. The first test comparing U_3Si with U_3Si_2 proved that U_3Si_2 had lower swelling than U_3Si. Then, a series of tests explored swelling, interaction layer thickness, and corrosion for qualification.

2.2 Fuel swelling by fission products

Dividing fuel swelling by fission products into two separate sections is convenient. Solid fission products create the volume difference between uranium and solid products. At the same time, gaseous products such as Xe and Kr generate bubbles, and swelling results from the addition of solid and gaseous products. The swelling level is a function of temperature, burnup, and irradiation density for temperatures below 250 °C. Solid fission products induce precipitates, creating crystal damage; the swelling for solids is around four times the fission densities. The swelling became trouble for high fission densities beyond 3×10^{27} fissions/m^3. Thus, it reduces the thermal conductivity of the fuel plate, increasing the temperature gradient. The irradiation-enhanced defect concentrations drive fission gas diffusion. After the curve knee, the fission gas released speeds up the loss of the mechanical properties of the plate. The swelling curve exhibits a sharp knee that shifts to a higher fission density. The knee of the curve occurs because of the rapid multiplication of the gas bubble, and the bubble size increases linearly. UMo surfaces. The swelling rate is given as a function of fission densities and molybdenum content in the weight of U-Mo. Equations (1) and (2) represent swelling.

$$for\ f \le 2.0\times10^{21}$$

$$\frac{\Delta V}{V} = 5.8336\times10^{-23}.(1.25 - 2.5W_{Mo}).f \quad (1)$$

$$for\ f \ge 2.0\times10^{21}$$

$$\frac{\Delta V}{V} = (1.25 - 2.5W_{Mo}).[(0.1667\times10^{-22}).(f - 2.0\times10^{21})] \quad (2)$$

where $\Delta V/V$ represents the fuel swelling for the U-Mo alloy, W_{omb} is the weight fraction of Mo in the fuel alloy, and f represents the fission density (fissions/cm^3).

Irradiation tests executed in RERTR-6 show that adding 2–5 wt% silicon to the Al-4043 reduces U-7Mo dispersion drawbacks. They drastically altered the composition of the (U-Mo-Al-Si) zone, reducing irradiation growth. Figure 6 illustrates U-MO swelling.

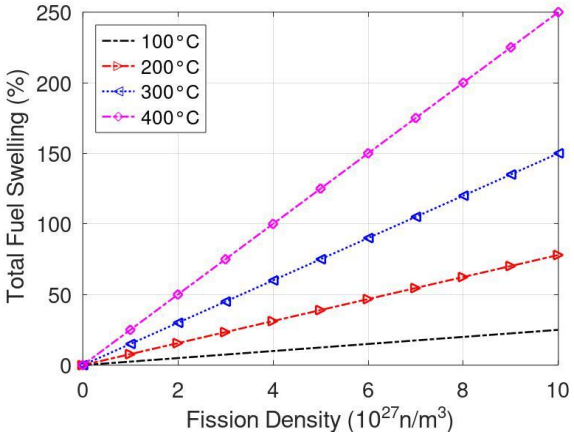

Figure 6. Swelling of the U-Mo fuel plate versus irradiation temperature.

However, the thickness layer grows more slowly in U-7Mo/Al dispersions with 8.8 gU/cm^3 using Al-6061 cladding. Figure 7 demonstrates uranium loading versus the fission phase percentage.

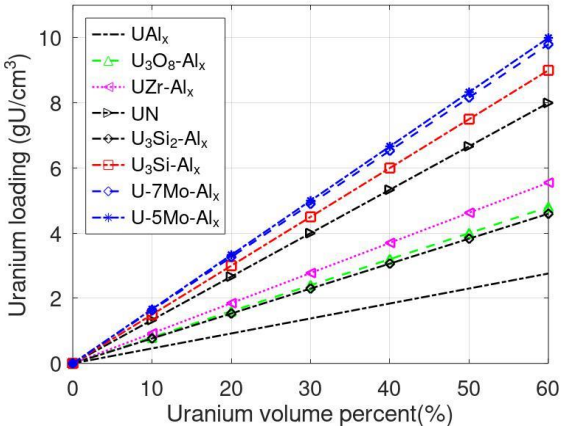

Figure 7. Uranium loading versus fission phase percents.

Equation (3) represents an empirical correlation for U-xMo fuel given as a function of the fission and fraction of molybdenum in weight.

$$y^2 = 2.2443 \times 10^{-19}(1.625 - 6.25W_{Mo}).\left((f^{0.75})\right).\Delta t.\exp\{(-10000|R.T)\}. \quad (3)$$

where y is the interaction thickness (cm), W_m is the weight fraction of Mo in the fuel alloy, f is the fission rate density (fissions/cm^{3}s), Δt is time (seconds), R represents the gas constant (1.987 cal/mol-K), and T is the temperature (K).

3. CRITICAL FLOW VELOCITY FOR COLLAPSING

The International Atomic Energy Agency accounts for 223 research reactors in operation across 53 nations, according to the Research Reactor Database. Research reactor plates are significantly longer than they are thick, with a thickness of the order of millimeters. The parallel in the fuel element assembly creates channels with a few millimeters of thickness between them for the coolant to pass through. Large permanent plate deflections at critical velocity obstruct the reactor core's flow channel and cause plate overheating. Core design often needs a high flow velocity to ensure the cooling of the fuel plate. Increasing fuel plate vibration brought the collapse of the flow channels. Dispersion fuel plates have a particular shape and comprise thin, curved, or flat plates. The cooling fluid then passes through a few millimeter-thick channels. Then, the pressure-unbalance forces developed by a slight deflection exceed the corresponding elastic restraining forces, and the plates collapse. Figure 8 depicts a hypothetical plate fuel arrangement.

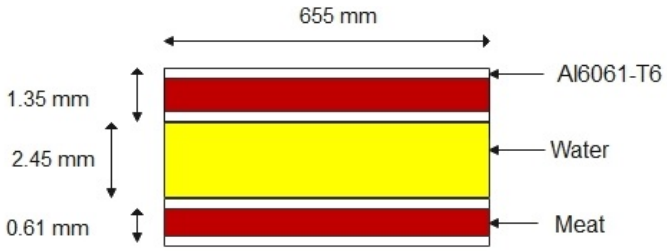

Figure 8. Plate fuel dimensions and water channel.

Early 1960s investigations found that the plates might become unstable when the flow rate increased. The collapse happened in tests conducted at Oak Ridge, generating Miller's formulation. However, studies from the 1970s suggest that the boundary conditions affect the type of instability, whether static or dynamic. The flat plates suffered plastic damage, and the curved plates buckled, inducing mechanical deformation throughout their long length and mechanical strain over their thin thickness. Miller's formulation determines the top speed at which flow-induced vibrations deform and collapse. Equation (4) depicts Miller's critical flow velocity (Jensen & Marcum, 2014).

$$Vc = \left(\frac{15.E.Ta^3.Th}{\rho.Tb^4.(1-\nu^2)}\right)^{0.5} \quad (4)$$

where E is the elastic moduli in (Pa), Ta is the plate thickness in (m), Tb is plate width in (m), Th is the flowing channel height, ρ is the coolant density (kg/m^3), and ν is the Poison ratio.

However, mechanical parameter uncertainties significantly affect the critical velocities' safety margins. Table 4 shows typical parameters used in a hypothetical research reactor. Figure 9 depicts the critical flow velocity based on the Miller formulation.

Table 4. Research reactor parameters used for calculating critical flow velocity.

Plate fuel properties	**Miller parameters**
Elastic modulus of Al 6061-T6 (GPa)	68.9
Plate thickness (mm)	1.35
Plate width (mm)	70.5
Poisson's ratio Al 6061-T6	0.33
Channel height (mm)	2.45
Water coolant density (kg/m^3) at 25°C	998
Water dynamic viscosity (mPas)	88.7

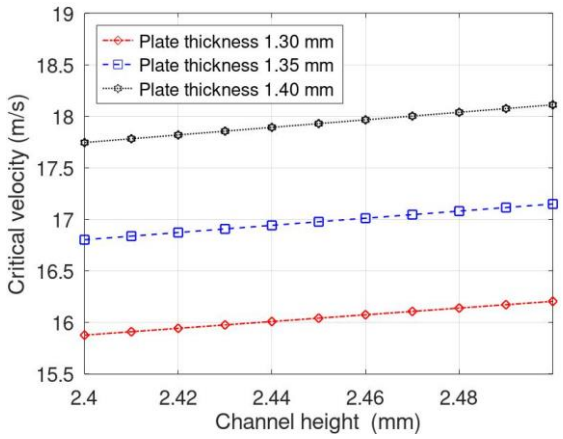

Figure 9. Critical flow velocity using the Miller formulation as a function of channel height.

The plates collapsed when the velocity reached 0.9 to 1.9 of the Miller critical velocity. Besides, the channel has a pressure drop depending on the fluid velocity. Figure 10 depicts the pressure drop given as a velocity function.

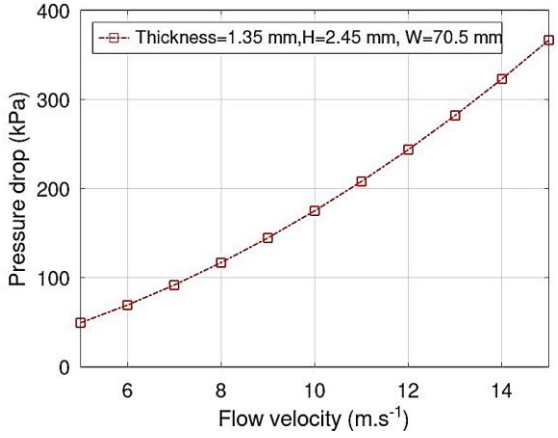

Figure 10. Pressure drop for different fluid flow velocities.

The flow-induced deflection phenomenon is a magnification of built-in channel spacing perturbations. The deflections assume a sine wave shape along the long axis of the channel. At high flow rates, around 1.9 times the collapse velocity, adjacent plates always move in opposition, opening and closing coolant channels. Observed deflections over the critical velocity were enough to bring adjacent plates into contact and close flow channels.

Plate deflections can obstruct the flow in the reactor core and result in plate overheating. Using the Bernoulli theorem employed for incompressible flow, one can calculate the pressure difference across parallel plates. The pressure drop across the fuel element comes from the flow channel of the contraction at the entrance.

Also, there is an expansion next to the parallel and output plates. We need to use the Colebrook formula to calculate the pressure drops to limit the friction factors. The friction factor reduces with increasing velocity; measured at a speed of 5 m/s, it is 0.024; when we reach 14 m/s, the pass factor is 0.020. As the channel height increases, assuming a fixed plate thickness, the Reynolds number also increases. A plate with a 1.35 mm thickness can modify the Reynolds number, which varies when the channel height is 2.40 mm, which equals 87,721. When the channel height reaches 2.50 mm, Reynolds reaches 93,133. Figure 11 illustrates critical flow velocity as a function of Reynolds number.

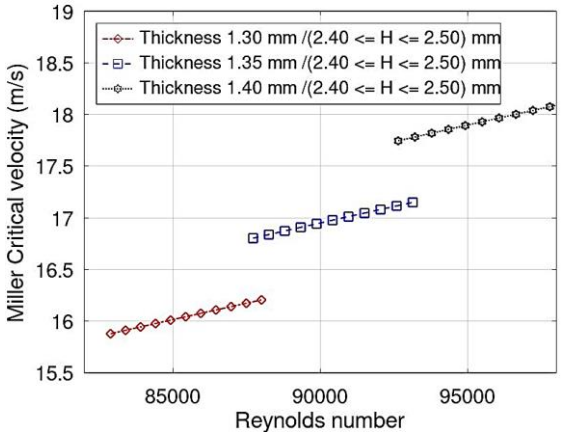

Figure 11. Critical flow velocity is given as a function of Reynolds number.

4. CONCLUSION

The RERTR program followed the M3 plan to promote technical advances in LEU fuel. Soon, the global effort will merge the monolithic U-10Mo alloy with aluminum cladding. Monolithic fuel plates contain a Zr diffusion barrier between the U-10Mo fuel and Al-6061 cladding that suppresses the interaction between the U-Mo fuel foil and Al alloy cladding, which is a drawback under irradiation. Intermetallic compounds such as U-Mo, U-Al, U_3Si_2, or U3Si and ceramics dispersed in an aluminum matrix formed the fuel plates. Each generation presents a greater density of uranium, reaching 18 gU/cm^3 for monolithic U-10Mo. Since 1978, it has converted most HEU reactors to LEU, including medicine isotope producers dedicated to the molybdenum-99 (Mo-99) supply chain, which still works with UAl_x targets with high enrichment.

5. ACKNOWLEDGMENT

The Energy and Nuclear Research Institute (IPEN/CNEN) sponsored this work, and the author is grateful for the motivation that assisted in this research.

6. REFERENCES

Bobkov, V., et al., 2008, "Thermophysical properties of materials for nuclear engineering: a tutorial and collection of data." IAEA, Vienna.

Copeland, G. L., & Martin, M. M., 1982. Development of High-Uranium-Loaded U_3O_8-Al Fuel Plates. Nuclear Technology, vol. 56(3), pp. 547–552.

Frazer, D., Maiorov, B., Carvajal-Nuñez, U., Evans, J., Kardoulaki, E., Dunwoody, J., & White, J. T., 2021. High-temperature mechanical properties of fluorite crystal structured materials (CeO_2, ThO_2, and UO_2) and advanced accident-tolerant fuels (U_3Si_2, UN, and UB_2). Journal of Nuclear Materials, vol. 554, pp. 153035.

Gan, J., Keiser Jr, D. D., Miller, B. D., Jue, J. F., Robinson, A. B., Madden, J. W., & Wachs, D. M., 2011. Microstructure of the irradiated U_3Si_2/Al silicide dispersion fuel. Journal of Nuclear Materials, vol. 419(1-3), pp. 97–104.

Hofman, Gerard L., 1998. Design of high-density gamma-phase uranium alloys for LEU dispersion fuel applications. *No. ANL/TD/CP-97494*. Argonne National Lab., IL (US).

Iltis, X., Havette, J., Klosek, V., Onofri, C., Lee, K. H., Kim, J. H., & Palancher, H., 2023. Microstructural characterization of atomized U_3Si_2 powders with different silicon contents (7.4–7.8 wt%). Journal of Nuclear Materials, vol. 573, pp.154141.

Jian, X., & Ding, S., 2020. Thermal creep effects of aluminum alloy cladding on the irradiation-induced mechanical behavior in U–10Mo/Al monolithic fuel plates. Nuclear Engineering and Technology, vol. 52(4), pp. 802–810.

Jensen, P., and Marcum, W. R., 2014. Predicting critical flow velocity leading to laminate plate collapse flat plates. Nuclear Engineering and Design vol. 267 pp 71–87.

Kim, Y. E., Park J. W. Park, Cleveland J., 2006. "Thermophysical properties database of materials for light water and heavy water reactors." International Atomic Energy Agency, Vienna, Austria, Tech. Rep. IAEA-TECDOC-1496.

Kim, Y. S., & Hofman, G. L., 2011. Interdiffusion in U_3Si–Al, U_3Si_2–Al, and USi3–Al dispersion fuels during irradiation. Journal of nuclear materials, vol. 410(1–3), pp. 1–9.

Kniznik, L., Alonso, P. R., Gargano, P. H., & Rubiolo, G. H., 2011. Simulation of UAl_4 growth in an UAl_3/Al diffusion couple. Journal of Nuclear Materials, vol 414(2), pp. 309–315.

Konings, R., & Stoller, R. E., 2020. *Comprehensive nuclear materials*. Elsevier.

Leenaers, A., Parthoens, Y., Cornelis, G., Kuzminov, V., Koonen, E., Van den Berghe, S., & Schulthess, J., 2017. Effect of fission rate on the microstructure of coated UMo dispersion fuel. Journal of Nuclear Materials, vol. 494, pp. 10–19.

Mariani, R. D., Nelson, A., Blomquist, R., Keiser Jr, D. D., Youinou, G. J., Hofman, G., & Griffith, G. W., 2020. "Initial Evaluation of Fuel-Reactor Concepts for Advanced LEU Fuel Development" (No. INL/EXT-20-54641). (INL), (ORNL),(ANL). (United States).

Mei, Z. G., Miao, Y., Liang, L., & Yacout, A. M., 2019. First-principles study of surface properties of uranium silicides. Journal of Nuclear Materials, vol. 513, pp. 192–197.

Park, J. M., Ryu, H. J., Oh, S. J., Lee, D. B., Kim, C. K., Kim, Y. S., & Hofman, G. L., 2008. Effect of Si and Zr on the interdiffusion of U–Mo alloy and Al. Journal of Nuclear Materials, vol. 374(3), pp. 422–430.

Pioro, I. (Ed.). 2022. Handbook of Generation IV Nuclear Reactors: A Guidebook. Woodhead Publishing.

Rest, J., Kim, Y. S., Hofman, G. L., Meyer, M. K., & Hayes, S. L., 2006. U-Mo fuels handbook. Version 1.0 (No. ANL-09/31). Argonne National Lab.(ANL), Argonne, IL (United States).

Van den Berghe, S., Leenaers, A., Koonen, E., & Sannen, L., 2011. From high to low-enriched uranium fuel in research reactors. Advances in Science and Technology, vol. 73, pp. 78–90.

Wang, X. S., & Xu, Y., 2004. Experiments, characterizations, and analysis of a U_3Si_2–Al dispersion fuel plate with sandwich structure. Journal of nuclear materials, vol. 328(2–3), pp. 243–248.

Williams, A. F., B. W. Leitch, and N. Wang., 2013 A microstructural model of the thermal conductivity of dispersion type fuels with a fuel matrix interaction layer. Nuclear Engineering and Technology, vol. 45.7 pp: 839–846.

Wilson, E. H., Jaluvka, D., Hebden, A. S., Stillman, J. A., & Jamison, L. M., 2019. US High-Performance Research Reactor Preliminary Design Milestone for Conversion to Low-Enriched Uranium Fuel. Argonne National Lab.(ANL), Argonne, IL (United States).

Yang, G., Liao, H., Ding, T., & Chen, H., 2021. Preliminary study on the thermal-mechanical performance of the U_3Si^2/Al dispersion fuel plate under normal conditions. Nuclear Engineering and Technology, vol. 53(11), pp. 3723–3740.

7. RESPONSIBILITY NOTICE

The author is the only person accountable for the printed materials used in this work.